Journal of Oil Palm Research
DOI: https://doi.org/10.21894/jopr.2023.0011

THERMAL ANALYSIS AND NON-ISOTHERMAL THERMOGRAVIMETRIC KINETICS ANALYSIS USING COATS-REDFERN METHOD OF A TORREFIED EMPTY FRUIT BUNCHES

MOHAMAD AZRI SUKIRAN[1]*; PETER ADENIYI ALABA[2]; ABU BAKAR NASRIN[1]; ASTIMAR ABDUL AZIZ[1] and SOH KHEANG LOH[1]

ABSTRACT

Thermal and mechanistic behaviours of solid biofuel are essential for commercial exploitation. In this work, the suitability of torrefied EFB as a solid biofuel was evaluated by investigating its physicochemical characteristics, kinetics and reaction mechanism during pyrolysis. The pyrolysis behaviour of raw and torrefied EFB was predicted via thermogravimetric analysis, kinetic parameters via Coats-Redfern three pseudo-components model-fitting method and pyrolysis mechanism via Criado method with Z-master plot. The physicochemical properties of torrefied EFB improved significantly compared to raw EFB in terms of fuel properties such as carbon content (8%-41%), fixed carbon (79%-328%) and calorific value (7%-42%). The degradation rate of hemicellulose and cellulose of torrefied EFB increased when the torrefaction temperature increased from 225°C to 300°C, leading to lower char yield and overall activation energy to initiate the pyrolysis process. The model deduced that higher overall activation energy was exhibited by raw EFB (9.39 kJ/mol) than those of torrefied EFB ranging from 6.55-7.86 kJ/mol (300°C-225°C). Thermal degradation of hemicellulose from torrefied EFB dominated the process by about 74% compared to cellulose and lignin when torrefaction temperature increased from 225°C to 300°C. Torrefaction could convert the power law mechanism to nucleation and growth mechanism gradually, allowing for better EFB thermal decomposition as a whole.

Keywords: activation energy, empty fruit bunches, kinetic reaction mechanism, pyrolysis, torrefaction.

Received: 28 June 2022; **Accepted:** 8 January 2023; **Published online:** 9 March 2023.

INTRODUCTION

Every year, more than 100 million tonnes (wet basis) of oil palm biomass will be generated in the form of empty fruit bunches (EFB), palm kernel shells, mesocarp fibre, oil palm trunks and oil palm fronds. Of these, EFB is the most abundantly available, at the amount of ≈ 21.61 million tonnes (wet basis), from the processing of 96.09 million tonnes of fresh fruit bunches at 457 palm oil mills in 2020 (Parveez *et al.*, 2021). According to Chang (2014), EFB is generally 3.5 kg in mass and has a thickness of up to 130 mm and 300 mm in width and length. It usually encompasses a considerable amount of moisture, up to 70 wt.% due to sterilisation by steam during oil processing which is a natural way for fruit maturation (Loh, 2017; Sukiran *et al.*, 2020). Although EFB contains a substantially higher amount of holocellulosic components, 78 wt.% in total from cellulose and hemicellulose (Loh, 2017), which are

[1] Malaysian Palm Oil Board,
6 Persiaran Institusi, Bandar Baru Bangi,
43000 Kajang, Selangor, Malaysia.

[2] Department of Chemical Engineering,
Faculty of Engineering, University of Malaya,
50603 Kuala Lumpur, Malaysia.

* *Corresponding author e-mail: azri@mpob.gov.my*

more suitable for bioconversion compared to lignin (~20 wt.%), its high moisture and oxygen contents coupled with low energy density and calorific value (CV) have hindered the use of EFB as biofuel in its natural form. As EFB is not readily usable, it is therefore important to subject it to thermochemical pretreatment through pyrolysis, gasification and combustion before the biomass is turned into an easy-to-use biofuel.

Although pyrolysis is promising for biomass conversion into bio-oil, bio-char and combustible gas, it has several drawbacks. In the pyrolysis process, the bio-oil obtained exhibits some inferior properties: High water content and acidic value, poor volatility, low heating value and chemically unstable with the undesired aging problem. These characteristics hamper the direct and efficient utilisation of bio-oil as biofuel and fine chemicals. All the above-mentioned problems are caused by the low quality of biomass, hence pretreatment is necessary in order to improve the fuel properties (Abnisa and Alaba, 2021). Among the biomass pretreatment methods developed, torrefaction is an effective approach to reduce oxygen content and increase bulk density, *i.e.*, the key quality determinants of biomass feedstocks for pyrolysis.

Torrefaction is a thermochemical technique in biomass conversion at between 200°C and 300°C for 10-60 min in an inert atmosphere (Zhang *et al*., 2021). The chemical properties of biomass such as O/C and H/C ratios will improve due to the removal of hydroxyl and organic volatiles and the decomposition of hemicellulose during the torrefaction process. Thus, torrefied biomass is deemed to have superior properties similar to coal for the ease of handling, milling and transporting. The improvement made after the torrefaction process renders the torrefied biomass suitable to be used as a feedstock for the pyrolysis process. The resultant bio-oil will be associated with an increased fixed carbon content and reduced volatile matter. In addition, torrefaction prior to pyrolysis can subsequently increase the CV and decrease the acidity of bio-oil (Fleig *et al.*, 2021).

Thermogravimetric analysis (TGA) is the most common and simplest method of evaluating the kinetics of pyrolysis (Alaba *et al.*, 2020). TGA summarises the pyrolysis characteristics based on a kinetic model and shows the variation in activation energy. Many literatures can be found related to the pyrolysis kinetics of biomass using TGA (Kumar Mishra and Mohanty, 2021; Sharma and Sheth, 2018). For example, Müller-Hagedorn and Bockhorn (2007) studied the TGA behaviour of wheat and barley straw during pyrolysis. The formal kinetic parameters for the pyrolysis of the main components (hemicelluloses, lignin and cellulose) and their degradable amounts were modelled by assuming parallel, independent reactions. Damartzis *et al.* (2011) performed non-isothermal TGA behaviour of cardoon (*Cynara cardunculus*) stems and leaves. Three different kinetic models - the independent parallel reaction model, Kissinger-Akahira-Sunose (KAS) and Ozawa-Flynn-Wall (OFW) were evaluated for the kinetic parameters of the process. Meanwhile, Li *et al*. (2008) studied the thermal degradation kinetics of the main constituents of different parts of corn using two different three pseudo-component models.

On the other hand, several studies on the pyrolysis kinetics of oil palm biomass have been reported. Mohamed *et al.* (2018) modelled the kinetics of thermogravimetric catalytic pyrolysis of EFB with alumina using KAS and OFW. The presence of a catalyst increased the activation energy values of EFB pyrolysis. Soh *et al*. (2019) calculated pyrolysis kinetics parameters of oil palm biomass using Coats-Redfern integral method and Šesták-Berggren function to determine the activation energy and reaction mechanism. The activation energy of oil palm biomass pyrolysis during hemicellulose decomposition was found lower relative to the cellulose counterpart. Meanwhile, Kasim *et al*. (2018) applied the Coats-Redfern to model decomposition kinetics of raw and torrefied EFB to estimate the activation energy and pre-exponential factor. Both the kinetics parameters of torrefied EFB were higher than that for pyrolysis of EFB.

All these studies provide remarkable insights into understanding the fundamental reaction mechanisms and reaction kinetics of biomass pyrolysis, ranging from simple single-step kinetic model to a more complex reaction model. However, very few literature studies have examined the pyrolysis kinetics of torrefied biomass using multi pseudo-component (cellulose, hemicellulose and lignin) models (Brillard *et al.*, 2020; Singh *et al.*, 2019) Hence, there is a need for more in-depth understanding on thermal degradation of individual fibre component and also as a whole, for biofuel thermal conversion in particular. Therefore, this study aimed to fill this gap by investigating the thermal kinetics degradations of three pseudo-components of torrefied EFB by the Coats-Redfern method. The use of kinetic analysis to quantify the main lignocellulosic fractions allows for the inclusion of restrictions for a more precise quantification, while a physical interpretation can be added to the deconvolution process.

In this study, torrefaction of EFB commenced in a fixed bed reactor under nitrogen atmosphere at different temperatures (225°C, 250°C, 275°C and 300°C) for 30 min. TGA data of raw and torrefied EFB were used to predict the pyrolysis behaviour and estimate kinetic parameters using Coats-Redfern method with an assumption of three pseudo-components. In addition, the pyrolysis reaction mechanism of raw and torrefied EFB as predicted

using the Criado method with a Z-master plot, was new and not reported elsewhere for torrefied biomass pyrolysis. The approach used in this study offered a more reliable kinetics modelling, contributing to the design and simulation of torrefied biomass pyrolysis.

MATERIALS AND METHODS

Material Preparation

The raw material, EFB was collected from a palm oil mill located at Labu, Negeri Sembilan, Malaysia. The samples were milled to reduce their sizes and screened to obtain particle sizes within 0.1-1.0 mm. The resulting particles of EFB were dried at 103ºC for 24 hr until constant weight was achieved.

Torrefaction Experiment

The torrefaction of EFB was carried out in a vertical fixed bed reactor as the illustrated in *Figure 1*. The detailed procedure of torrefaction experiment has also been shown in our previous study (Sukiran *et al.*, 2021). A quartz reactor containing about 20 g of raw EFB was placed in the centre of furnace. After the equipment was assembled, nitrogen was used to exhaust the air inside the quartz reactor, and the gas was continuously introduced to maintain an inert environment. EFB samples were heated at a heating rate of 10°C/min until the desired torrefaction temperature namely 225°C, 250°C, 275°C and 300°C was reached, and maintained for 30 min of residence time. While vapour released from the process was condensed by a condenser and collected as a liquid product, a solid product (torrefied EFB) remaining inside the reactor was also collected. Both the products were weighed to obtain their mass yields based on Equation (1):

$$\text{Mass yield (wt.\%)} = \frac{\text{Mass of the desired product (liquid/solid)}}{\text{Mass of raw EFB}} \times 100\% \quad (1)$$

The gas yield was calculated by subtracting the mass yield (wt.%) of liquid and torrefied EFB from the total of 100%. The torrefaction experiment at each temperature was repeated three times to ensure experimental repeatability.

Characterisation of Raw and Torrefied EFB

The proximate analyses of raw and torrefied EFB were conducted to determine moisture content, volatile matter, fixed carbon and ash content according to ASTM D5142 (ASTM, 1998) using a thermogravimetric analyser (LECO TGA-701). LECO CHN 628 and LECO S 628 were used to determine carbon, hydrogen, nitrogen and sulphur contents according to ASTM D5373 (ASTM, 2014). Temperature and time of the combustion for CHN 628 ranged from 850°C to 950°C within 3 min, meanwhile combustion analysis for sulphur was set at 1350°C within 2 min. The oxygen content was determined from the difference between 100% and the total percentage of carbon, hydrogen, nitrogen and sulphur. The changes in the atomic composition of EFB were established using the Van Krevelen diagram. It was constructed using the molar ratio of

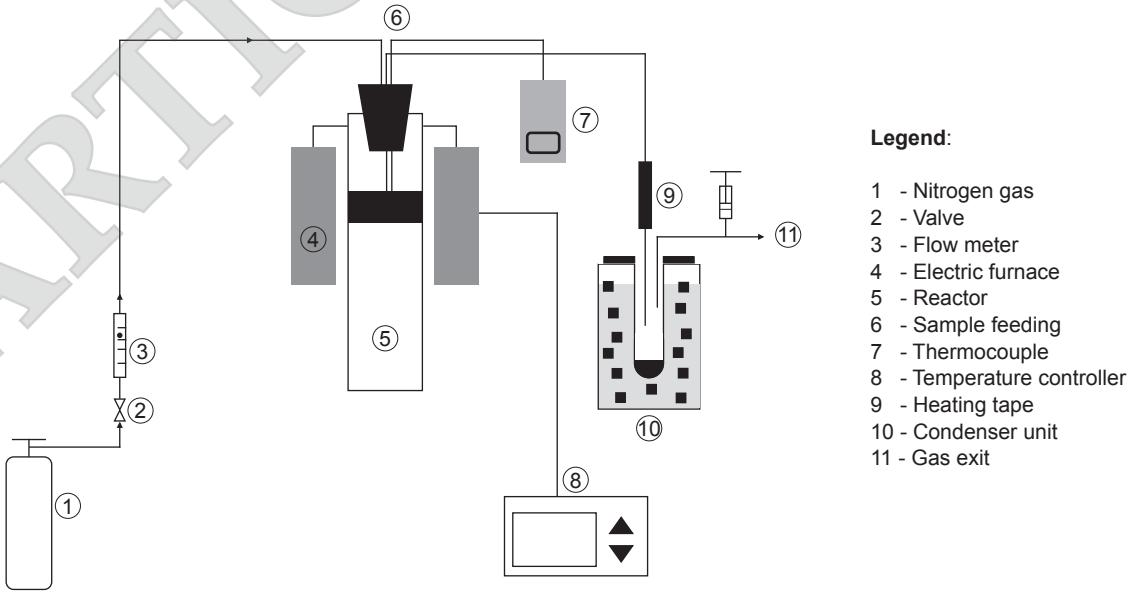

Figure 1. Schematic diagram of experimental setup for torrefaction of empty fruit bunches.

hydrogen: Carbon (hydrogen index) as the ordinate to the molar ratio of oxygen: Carbon (oxygen index) as the abscissa. The CV of raw and torrefied EFB were determined using a bomb calorimeter (LECO AC-600) according to ASTM D5865-07 (ASTM, 2019). The chemical compositions of the raw and torrefied EFB were analysed according to ASTM 1104-56 (ASTM, 1978a) and ASTM D1103-60 (ASTM, 1978b) for holocellulose and α-cellulose, respectively.

Briefly, a composite of cellulose and hemicellulose was extracted from raw and torrefied EFB using acidified sodium chlorite method. Approximately 24.0 g of sample was mixed with 960 mL distilled water and treated with 3.0 mL acetic acid and 9.0 g sodium chlorite at 70°C-80°C for 4 hr under continuous stirring. The mixture was then washed with hot water, filtered and dried at 105°C for 24 hr. Determination of holocellulose was carried out using dry weight method. A total of 12.0 g of dried holocellulose obtained was further dissolved in 240 mL of 17.5% (v/v) NaOH solution and stirred for 30 min. A total of 60 mL of NaOH solution was added into the mixture and allowed to mix to separate hemicellulose from the holocellulose and leaving α-cellulose. The insoluble α-cellulose was filtered and washed separately with 8.3% (v/v) NaOH solution followed by 10.0% (v/v) acetic acid. The α-cellulose was finally washed with hot water to a neutral pH and dried overnight at 80°C. The hemicellulose content was calculated as the difference in the weights of α-cellulose and holocellulose. The lignin content was determined using the gravimetric method according to TAPPI T222 om-11 (TAPPI, 2011). A 0.5 g sample was weighed into a 100 mL Erlenmeyer flask and stirred for 2 hr in 10 mL of cold 72.0% (v/v) H_2SO_4 solution. The mixture was transferred into a 500 mL beaker and boiled for 4 hr in 300 mL distilled water under continuous stirring. The mixture was filtered off using glass microfibre filter grade GF/B (Whatman) in porcelain crucible. The residue retained on the filter was washed with hot water until it was acid-free and allowed to dry at 105°C for 2 hr and weighed. Based on the obtained mass yield and CV of torrefied product, energy yield (E_y) was calculated as Equation (2):

$$E_y = \text{Mass yield of torrefied EFB} \times \left[\frac{\text{CV of torrefied EFB}}{\text{CV of raw EFB}}\right] \quad (2)$$

Pyrolysis Experiment

The thermogravimetric analyser (Perkin Elmer-Pyris 6) was used to determine pyrolysis of raw and torrefied EFB at different temperatures. In the experiment, an inert environment was created using high-purity nitrogen at 0.1 L/min using 10 mg of samples. The samples were heated from 30°C to 800°C at heating rates of 20°C/min. The gas atmosphere was high-purity nitrogen, and the gas flow rate was 0.2 L/min to ensure a pyrolysis reaction. Degradation of raw and torrefied EFB samples was determined from the thermogravimetric curves established via TGA based on ASTM E1131 (ASTM, 2020). Each experiment was replicated three times to ensure the reproducibility of the results. The temperature for calibration of TGA was accomplished using melting point standards to ensure accurate data collection. In addition, the data obtained were used for kinetics analysis.

Kinetics Analysis

Generally, the decomposition rate is given by Equation (3).

$$\frac{dx}{dt} = K(T) f(x)^2 \quad (3)$$

where x is the degree of conversion, T is temperature and t is time. The conversion rate $\frac{dx}{dt}$ for pyrolysis at constant heating rate, $\beta = \frac{dT}{dt}$, could be written as:

$$\frac{dx}{dt} = \beta\frac{dx}{dT} = K(T) f(x) \quad (4)$$

Also, the degree of advance, x is:

$$x = \frac{w_0 - w}{w_0 - w_f} \quad (5)$$

where w_0, w_f and w refer to mass of samples at the beginning, end and time, t, respectively. Since mass loss is temperature dependent, $K(T)$ is often modeled by Arrhenius Equation (Alaba *et al.*, 2016).

$$K(T) = A \exp\left(-\frac{E_A}{RT}\right) \quad (6)$$

where R is the gas constant (8.314 J mol^{-1} K^{-1}), A is the frequency factor, per min, E_A is the activation energy, kJ/mol and T is the absolute temperature, K. Combination of Equation (3) and (4) gives:

$$\beta\frac{dx}{dT} A \exp\left(-\frac{E_A}{RT}\right) f(x) \quad (7)$$

The kinetic models employed to analyse the thermogrametric data was Coats-Redfern model. The integral model developed by Coats and

Redfern suggests the correct order leading to the best straight-line plot. Therefore, Equation (7) becomes:

$$\ln\left(\frac{g(x)}{T^2}\right) = \ln\left(\frac{AR}{\beta E_A}\right) - E_A/(RT) \quad (8)$$

Plotting $\ln(g(x)/T^2)$ versus $1/T$ results in a linear plot where the slope corresponds to $-E_A/R$ and the intercept gives $\ln(AR/\beta E_A)$. This gives the value of activation energy and Arrhenius constant/frequency factor. The overall conversion rate given by Equation (8) and overall activation energy (E_T) given by Equation (9) is the sum of the partial conversion rates and partial activation energy respectively, where Ci indicates the contribution factor of the volatile fraction produced from each component (hemicellulose, cellulose and lignin) in the following Equation (9) and (10):

$$\frac{d\alpha}{dt} = \sum_{i=1}^{3} C_i \frac{d\alpha_i}{dt} = C_1\frac{d\alpha_1}{dt} + C_2\frac{d\alpha_2}{dt} + C_3\frac{d\alpha_3}{dt} \quad (9)$$

$$E_T = \sum_{i=1}^{3} C_i E_i = C_1E_1 + C_2E_2 + C_3E_3 \quad (10)$$

Prediction of Reaction Model

The model for solid-state reaction during pyrolysis of torrefied EFB was investigated by Z-master plot associated with Criado method (Equation 11) (Criado, 1978).

$$\frac{Z(\alpha)}{Z(0.5)} = \frac{f(\alpha)\times g(\alpha)}{f(0.5)\times g(0.5)} = \left(\frac{T_\alpha}{T_{0.5}}\right)^2 \times \frac{(d\alpha/dT)_\alpha}{(d\alpha/dT)_{0.5}} \quad (11)$$

Equation (11) was employed to generate the master plots equivalent to various solid-state reaction mechanism. The term [f(α) × g(α)/f(0.5) × g(0.5)] gives a theoretical curve, which signifies the characteristics of each reaction mechanism. On the other hand, the term [$(T_\alpha/T_{0.5})^2$ × $((d\alpha/dT)_\alpha/(d\alpha/dT)_{0.5})$] is to be derived from a curve obtained from experimental values. The conversion value, α, is a value to define weight decomposition. The conversion rate is normally from 0 to 1.0. In most studies, the midpoint value (0.5) is used (Gogoi *et al.*, 2018; Luo *et al.*, 2021). The point α = 0.5 is considered as the reference point, where the standard master plots of each considered kinetic mechanism intersect each other corresponding to value of [Z(α)/Z (0.5)] =1. The predominant reaction mechanism of the thermal degradation of solids can be deduced by comparison of the theoretical and experimental master plots.

RESULTS AND DISCUSSION

Product Distribution

Figure 2 shows EFB's torrefaction products distribution namely solid (torrefied EFB), liquid and gas at different temperatures for 30 min. As shown, the yields of torrefied EFB decreased with increasing torrefaction temperature, *i.e.*, between 40.50-90.30 wt.%. As torrefaction temperature increases, the yield of torrefied EFB decreases as the result of extensive decomposition of cellulose, hemicellulose and lignin present in EFB. According to Zhang and Zhang (2019), as temperature exceeds 200°C, volatile materials are released along with other components such as moisture, CO, CO_2 and some condensable matters such as acetic acid. Hence, higher amounts of these compounds were released at the employed higher temperature range in this study, therefore the mass of the torrefied EFB reduced and lower solid yield obtained at the end of the torrefaction process. At this rate, the colour of the torrefied EFB changed from dark brown to black as the temperature increased. Although high yield of torrefaction does not indicate that the EFB in the reactor is fully converted, several approaches can be used for quality checking. Visual observation of the physical appearance of raw biomass and their torrefied products, normally from light brown (raw EFB) to dark brown and then black, will be indicative of conversion status as the temperature and residence time increase. In addition, comparison of fuel properties (carbon content and CV) can also be accomplished to ensure full conversion of the materials. In this study, both high yield of torrefied product and good fuel properties are desirable. The trend of mass reduction of torrefied EFB was consistent with other studies concerning torrefaction of pigeon pea stalk and bamboo (Singh *et al.*, 2020a). Maximum reduction in mass yields of torrefied EFB was 40.50 wt.% at 300°C. Contrarily, the yields of liquid and gas products derived from torrefaction of EFB increased with torrefaction temperature. When the temperature increased from 225°C to 300°C, the mass yields of liquid and gas products increased from 3.00 wt.% to 21.27 wt.% and 6.70 wt.% to 38.20 wt.%, respectively. The maximum gas yield was attainable at 300°C, *i.e.*, 38.20 wt.%. At this temperature, secondary decomposition mainly occurred forming lots of condensable vapours.

Characterisation of Torrefied EFB

Figure 3 shows the volatile matter, moisture content, fixed carbon and ash content of torrefied EFB at different torrefaction temperatures. The results indicated that the fixed carbon and ash contents of torrefied EFB increased when

torrefaction temperature increased from 225ºC to 300ºC. The fixed carbon of torrefied EFB increased from 18.3 wt.% to 43.8 wt.%, about 79%-328% increment as compared to the raw EFB. Higher content of fixed carbon means that the torrefied product can produce more heat with a longer combustion time (Nudri *et al.*, 2020). Meanwhile, the ash contents increased from 3.1 wt.% to 11.9 wt.% with increasing torrefaction temperature. The breakdown of carbon-hydrogen bonds during torrefaction resulted in volatile losses and further concentrated the ash content in the torrefied EFB. In contrast, the volatile matter and moisture contents of torrefied EFB decreased when torrefaction temperature increased. The volatiles decreased from 75.8 wt.% to 42.5 wt.% when torrefaction temperature increased from 225ºC to 300ºC. Huge reduction in volatile matter was due to the catalytic effect of inorganic minerals present in the biomass (Almeida *et al.*, 2010). Low volatile matter in biomass indicates stable combustion since volatile matter is reactive, which causes spontaneous, unstable, incomplete combustion and emission of smoke when present in high quantity (Nudri *et al.*, 2020).

Elemental analysis of the raw and torrefied EFB at 225°C, 250°C, 275°C and 300°C is shown in *Table 1*. As the torrefaction temperature increased from 225ºC to 300ºC, the carbon content of torrefied EFB increased whereas the hydrogen and oxygen contents decreased. Similar trend for other torrefied biomasses has been reported previously (Chiou *et al.*, 2015). The carbon in the raw EFB amounted to 42.8 wt%, which increased to 60.4 wt% when it was torrefied at 300ºC. This was consistent with the increase in the fixed carbon as shown in *Figure 3*. Meanwhile, the oxygen and hydrogen contents decreased from 47.0 wt.% to 33.7 wt.% and 6.0 wt.% to 4.9 wt.%, respectively. Reduction of oxygen and hydrogen in the torrefied EFB was dominated by dehydration reaction in the form of water vapor and volatile compounds such as CO and CO_2. The sulphur content of torrefied EFB was in the range from 0.05 wt.%-0.06 wt.%.

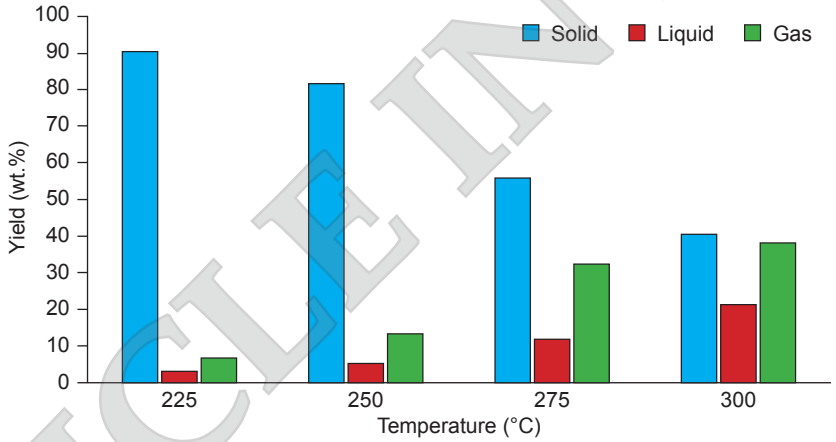

Figure 2. Torrefaction product distribution of empty fruit bunches at different temperatures.

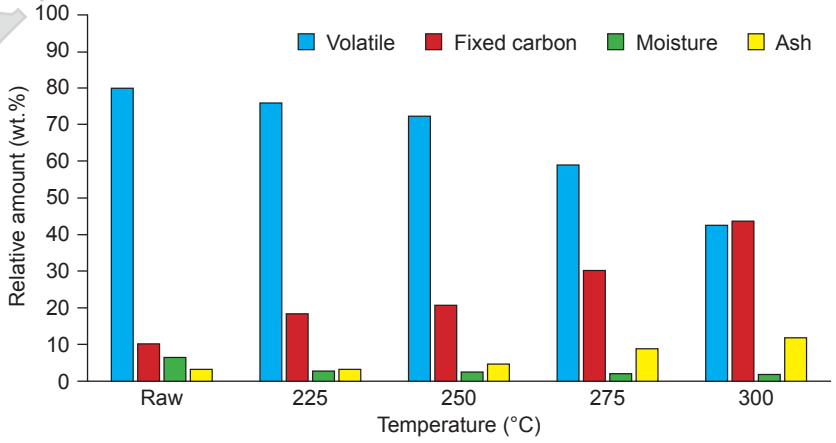

Figure 3. Proximate analysis of raw and torrefied empty fruit bunches at different temperatures.

Figure 4 shows the van Krevelen diagram for the raw and torrefied EFB at different temperatures. As can be seen, an increase in torrefaction temperature remarkably affected H/C and O/C atomic ratios. The H/C and O/C atomic ratios decreased from 1.70 and 0.89 (raw EFB) to 0.97 and 0.42 (torrefied EFB at 300°C), respectively. The decreases in the H/C and O/C ratios were mainly a result of the release of water and light volatile substances via dehydration, deoxygenation and dehydrogenation during torrefaction (Chen *et al.*, 2020). In addition, the atomic ratios of fossil-based coals such as lignite and bituminous were also illustrated in the same figure. As shown, the H/C and O/C atomic ratios of all the torrefied EFB were higher than those of lignite and bituminous; being that torrefied at 300°C the closest.

The CV of torrefied EFB was positively correlated with torrefaction temperatures, and vice versa for energy yield as listed in *Table 1*. The CV was in the range from 18.8 to 25.0 MJ/kg. This implies that the CV in the torrefied EFB increased by 7%-42% when compared to the raw EFB, due to the gradual increase of carbon content with torrefaction temperature. Similar trend of an increased CV for other torrefied biomasses has been reported previously (Wang *et al.*, 2018). Meanwhile, the trend of energy yield decreased significantly from 96.8% to 57.6% with increasing torrefaction temperature from 225°C to 300°C. Torrefied EFB with the least energy yield (57.6%) was generated at the most severe torrefaction conditions (300ºC), though with higher CV.

The chemical composition of the raw and torrefied EFB samples was determined to understand their conversion behaviour during torrefaction. *Figure 5* presents the chemical composition of the raw and torrefied EFB, namely, cellulose, hemicellulose and lignin. As shown in *Figure 5*, the cellulose content of raw EFB was higher than the hemicellulose and lignin contents. The high cellulose content in EFB is good for producing additional solid mass during the torrefaction process (Sukiran *et al.*, 2020). Not all celluloses are degraded to volatile products since the torrefaction process takes place at temperatures below 300°C, hence additional solid products are formed. Lignin is another component that is responsible for the major portion of the solid product in a thermal process. In *Figure 5*, the torrefaction process affected the lignocellulose components. As the temperature increases, the char yield decreases which could be associated with a higher degradation rate of hemicellulose, as indicated by the percentage of

TABLE 1. ULTIMATE ANALYSES, CALORIFIC VALUE AND ENERGY YIELD OF RAW AND TORREFIED EMPTY FRUIT BUNCHES AT DIFFERENT TEMPERATURES

Temperature (°C)	Ultimate analysis (wt. %)					CV (MJ/kg)	Energy yield (%)
	Carbon	Hydrogen	Nitrogen	Sulphur	Oxygen[a]		
Raw EFB	42.82	6.07	0.54	0.08	50.49	17.57	100
225	46.35	6.01	0.62	0.06	46.78	18.82	96.77
250	47.84	5.97	0.67	0.06	45.46	19.50	90.40
275	52.15	5.63	0.92	0.05	41.25	21.91	69.68
300	60.44	4.88	1.03	0.05	33.60	24.96	57.55

Note: [a]by difference.

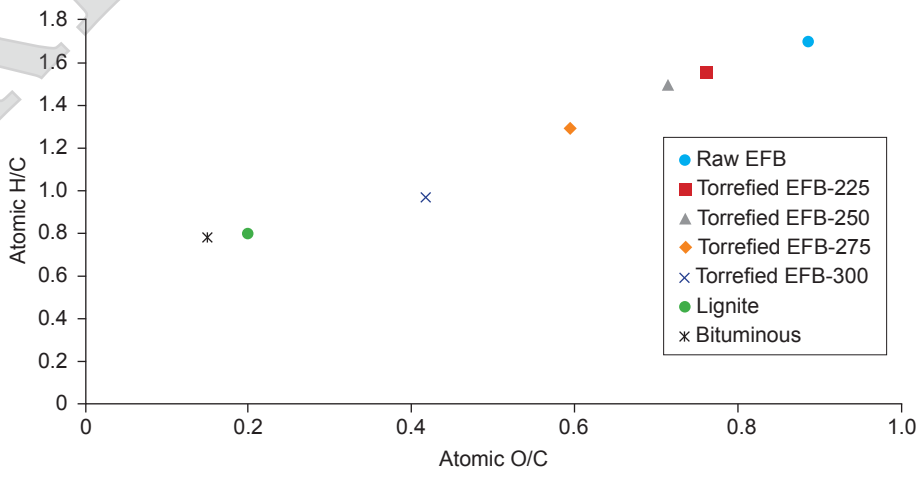

Figure 4. Van Krevelen plot of raw and torrefied empty fruit bunches (EFB) at various temperatures.

hemicellulose at different temperatures. Wang *et al.* (2017) obtained similar results during Norway spruce stem wood, stump and bark torrefaction. The hemicellulose content decreased significantly from 25.5% to 6.7% with increasing torrefaction temperature from 225°C to 300°C. After torrefaction at 275°C, more than half of the hemicellulose content in the EFB samples was degraded, while only a minor fraction occurring further at 300°C (6.7%). Decomposition of hemicellulose generated more CO_2, CO, water and oxygen-containing organic compounds during torrefaction (Chen *et al.*, 2018). The cellulose content of torrefied EFB decreased from 52.1% to 33.6% when the torrefaction temperature increased from 225°C to 300°C. Compared to hemicellulose content, the content of cellulose did not decrease evidently even at more severe torrefaction condition (300°C). At 225°C, the cellulose content was higher than that in the raw EFB. As severe degradation of hemicelluloses leads to a reduced mass, which further contributes to an increase of cellulose mass in totality of the EFB. The decomposed hemicellulose and cellulose further increased the lignin content of the torrefied EFB considerably with increasing torrefaction temperatures. The lignin content of torrefied EFB increased from 28.5% to 59.7%.

Thermogravimetric Analysis

The pyrolysis degradation behaviours of the raw and torrefied EFB at different temperatures and heating rate of 10°C/min are shown in *Figures 6a* and *6b*. The first stage was accompanied by elimination of water constituent and some light volatile compounds (Singh *et al.*, 2020b). As shown in *Figure 6a*, the peak value at the drying region (30°C and 150°C) became smaller and smaller when torrefaction temperature increased from 225°C to 300°C. This was expected as weight loss owing to moisture reduction for torrefied EFB was lesser than that of the raw biomass. Most water in the torrefied EFB samples had been removed as shown in *Figure 3*. For example, the weight loss of torrefied EFB at 250°C and 300°C were 8.1 wt.% and 10.0 wt.%, respectively as compared to the raw EFB, *i.e.*, 13.1 wt.%. The second stage was associated with devolatilisation process where major weight losses from EFB had occurred due to degradation of the hemicelluloses and celluloses. Such degradation took place between 200°C and 350°C, which was similar to our earlier finding (Sukiran *et al.*, 2017). As shown (*Figure 6a*), the shoulder on the lower temperature side during EFB torrefaction corresponded to thermal degradation of the extractives and also hemicellulose, which tend to decompose at much lower temperatures. Meanwhile, DTG curves (*Figure 6b*) show peaks of maximum degradation temperature for the EFB torrefied at 225°C, 250°C and 275°C. The peaks increased from 331°C to 337°C and to 344°C. The gradual increase in decomposition temperature of torrefied EFB might be due to total breakdown of hemicelluloses while retaining most of the celluloses and lignin. This phenomenon can be explained in *Figure 5*, where most hemicelluloses have been degraded along with a limited degradation of celluloses in the course of torrefaction. Thereafter, a continuous slight devolatilization occurred where lignin decomposition and char formation took place at temperature between 480°C and 700°C. As lignin is characterised by complex aromatic structure, its decomposition can only be accomplished with higher temperatures. Hence, the mass losses decreased slowly at this stage as shown in *Figure 6*. Besides, the inconsistency in thermal degradation of individual component of EFB contributed to deviation in residual char yield. The residual char yields after pyrolysis of the raw and torrefied EFB at 225°C, 250°C, 275°C and 300°C were 19.9%, 28.9%, 36.8%, 45.1% and 57.0%, respectively. The results correlated with the chemical compositions in *Figure 5*. The higher residual char yield in the torrefied EFB at higher pyrolysis temperature

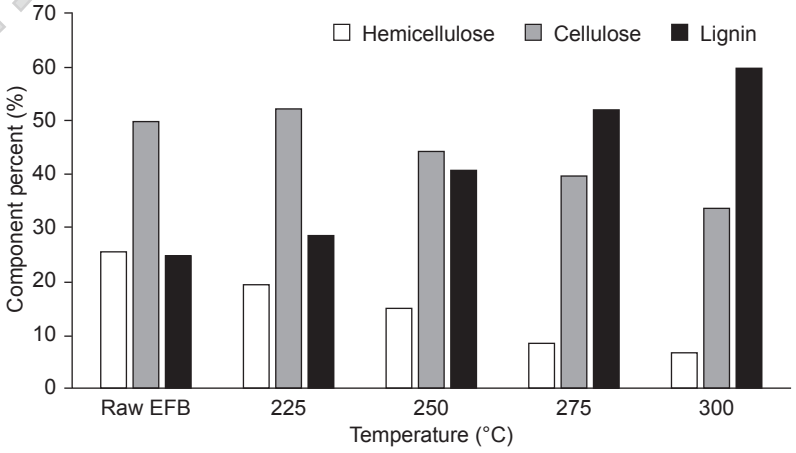

Figure 5. Chemical composition analysis of raw and torrefied empty fruit bunches at different temperatures.

was probably due to a larger mass of celluloses and lignin retained plus the cross-linkage reaction involved. At the end of the pyrolysis process, the mass rate curves exhibited small oscillations *(Figure 6b)* which corresponded to slow degradation of the lignin resided in torrefied EFB (Brillard *et al.*, 2020). Based on TGA and DTG (*Figure 6*), and chemical composition (*Figure 5*) analyses, the suitable torrefaction temperature to pre-treat EFB is 225°C-250°C, as for a more severe torrefaction condition a further loss of cellulose would significantly reduce bio-oil yield during pyrolysis.

Kinetics Analysis

Table 2 summarises the activation energy for individual hemicellulose, cellulose and lignin of the raw and EFB torrefied at different temperature (225°C, 250°C, 275°C and 300 °C). In this study, the respective activation energy was calculated using Coats and Redfern method based on Equation (8). As the torrefaction temperature increased from 225ºC to 300ºC, the activation energy of hemicellulose, cellulose and lignin decreased as shown in *Table 2*. Similar trend has been reported previously for other torrefied biomasses (Singh *et al.*, 2019). The overall activation energy, E_T also showed a similar downward trend with increasing torrefaction temperature. However, these values are much lower than those of other studies (Tian *et al.*, 2020), thus indicating that torrefied EFB is a promising feedstock for pyrolysis process as the energy required to initiate the reaction is lower. The E_T of the raw EFB is 9.39 kJ/mol compared to those of torrefied EFB, in the range of 6.55-7.86 kJ/mol (300°C-225°C). These values are low, probably due to the different reaction models used and their corresponding kinetics parameters which are sensitive to individual fibre composition. This finding is supported by a similar study using EFB as feedstock employing the Coats-Redfern model (Surahmanto *et al.*, 2020), where the activation energy obtained is equally low (7.58-12.63 kJ/mol), especially at higher temperature range (347°C-535°C). As shown in *Table 2*, the activation energy of hemicellulose resided in the torrefied EFB ranged from 4.07 (300°C) to 5.65 kJ/mol (225°C), compared to that of 5.79 kJ/mol (raw hemicellulose in EFB). The fact that hemicellulose becomes unstable at around 230°C has caused reduction in activation energy. Meanwhile, the value of activation energy for cellulose decreased from 7.05 (raw cellulose in EFB) to 5.63 kJ/mol (300°C) during torrefaction. At this high torrefaction temperature, the thermal stability of cellulose decreased (Singh *et al.*, 2019). The activation energy

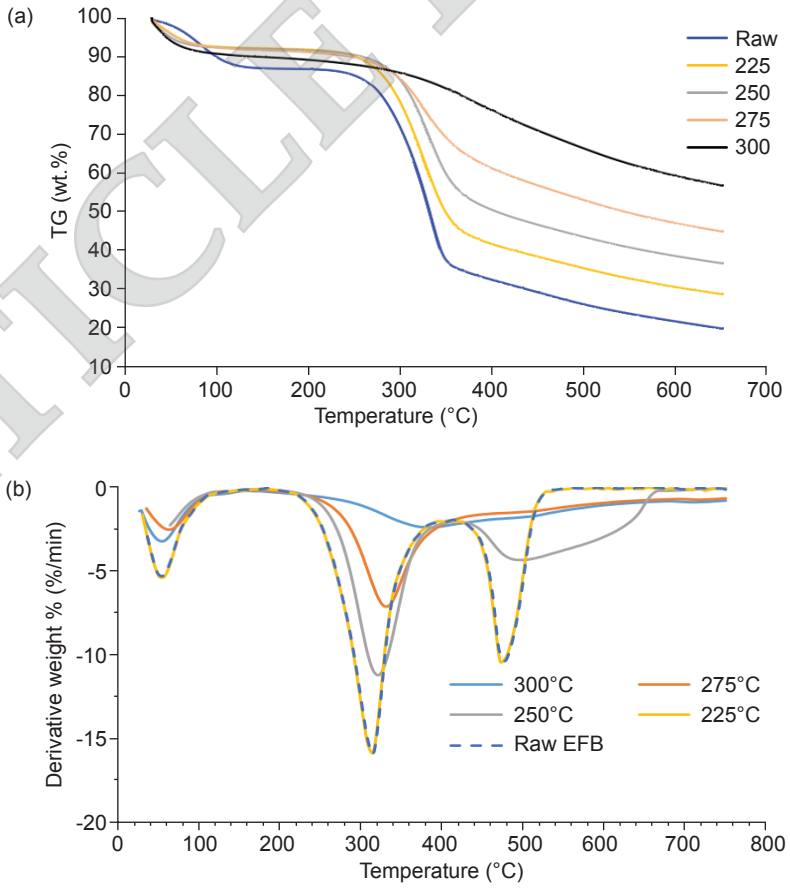

Figure 6. Experimental curves of (a) TGA and (b) DTG of raw and torrefied empty fruit bunches at different temperatures.

of lignin decreased from 12.89 kJ/mol (225°C) to 10.02 kJ/mol (300°C) indicating a more severe decomposition rate of lignin at higher torrefaction temperature.

Linear correlation equations obtained by Coats and Redfern plot method are given in *Table 2*. From the equations, it is clear that the slope of hemicellulose decreased significantly for torrefied EFB at 275°C, while for cellulose and lignin at 300°C. Contribution factor of hemicellulose for torrefied EFB decreased from 0.32 to 0.12 when torrefaction temperature increased from 225°C to 300ºC, confirming the thermal degradation of hemicellulose during torrefaction. Meanwhile, the contribution factor of cellulose for torrefied EFB at 300°C decreased significantly from 0.42 (raw) to 0.25, indicating that only this torrefaction temperature can efficiently remove cellulose. Higher cellulose content of EFB torrefied at lower temperatures will potentially generate higher volatile matters, leading to an increase in pyrolysis oil yield. In contrast, the contribution factor for lignin increased exponentially towards the end of EFB torrefaction at 300ºC, suggesting that most hemicellulose and cellulose had remarkably decomposed and thus the torrefied EFB was rich in lignin (Singh *et al.*, 2019). This observation is also reflected in *Figure 5*, which shows mostly hemicellulose degradation along with limited content of degraded cellulose during torrefaction.

Prediction of Reaction Mechanism

Criado analysis was used to determine the reaction mechanism during pyrolysis of the raw and torrefied EFB at a different conversion level and heating rate of 10°C/min. *Figure 7* presents the plots for the raw and torrefied EFB at α of 0.1 to 0.9.

Reaction mechanism at lower conversion (α<0.5). *Table 3* represents the decomposition mechanisms of the raw and torrefied EFB at temperature 225°C-300°C (denoted by EFB_T-225, EFB_T-250, EFB_T-275 and EFB_T-300). For raw EFB at conversion less than 0.5, the closest match with the theoretical curve is associated with D4 mechanism which corresponds to three-dimensional diffusion (Ginstling-Broushtein equation). Torrefied EFB_T-225 and EFB_T-250 follow power law (P4) mechanism; EFB_T-275 follows power law (P4) mechanism and nucleation and growth mechanism (4^{th} order Avrami-Erofeev model); EFB_T-300 follows power law (P3 and P4) mechanism and nucleation and growth mechanisms (3^{rd} and 4^{th} order Avrami-Erofeev model). Diffusion is the rate-determining step for the raw EFB probably due to the higher volatile content as shown in *Figure 3*. The thickness of product layer around EFB increases with increasing level of conversion. The forming of product layer could hinder the transfer

TABLE 2. KINETIC PARAMETERS FOR THE PSEUDO-COMPONENTS OF RAW AND TORREFIED EMPTY FRUIT BUNCH USING COATS AND REDFERN

Kinetic parameters	Raw_EFB	EFB_T-225	EFB_T-250	EFB_T-275	EFB_T-300
E_H (kJ/mol)	5.79	5.65	5.31	4.97	4.07
A_H	8.80E-06	8.58E-06	8.48E-06	8.32E-06	8.11E-06
R^2	0.94	0.90	0.93	0.93	1.00
C_H	0.36	0.32	0.28	0.26	0.12
Linear correlation equation for hemicellulose (ln(g(x)/T2 vs 1/T)	y = 896.72x - 14.275	y = 850.48x - 14.504	y = 712.07x - 14.347	y = 638.74x - 14.213	y =597.65x - 14.101
E_C (kJ/mol)	7.05	7.33	6.98	6.05	5.63
A_C	9.72E-06	9.88E-06	9.70E-06	9.74E-06	9.15E-06
R^2	0.94	0.91	0.91	0.93	1.00
C_C	0.42	0.55	0.52	0.44	0.25
Linear correlation equation for cellulose (ln(g(x)/T2 vs 1/T)	y = 848.24x - 14.372	y = 839.92x - 14.365	y = 838.94x - 14.345	y = 727.65x - 14.217	y = 677.46x - 14.208
E_L (kJ/mol)	13.53	12.89	12.68	11.65	10.02
A_L	7.46E-06	6.82E-06	6.89E-06	7.20E-06	7.66E-06
R^2	0.98	1.00	1.00	1.00	0.99
C_L	0.33	0.17	0.20	0.31	0.62
Linear correlation equation for lignin (ln(g(x)/T2 vs 1/T)	y = 1386.9x - 15.129	y = 1583.6x - 15.297	y = 1524.9x - 15.314	y = 1401.4x - 15.175	y = 1205.6x - 14.962
Overall activation energy (ET), kJ/mol	8.39	7.86	7.74	7.49	6.55

Note: $y = \ln(g(x)/T^2$ and $x = 1/T$; EFB T-XXX = EFB torrefied at XXX°C; H - hemicellulose; C - cellulose; L - lignin.

of heat from the surrounding. Therefore, all the torrefied EFB (EFB_T-225, EFB_T-250, EFB_T-275 and EFB_T-300) were not controlled by diffusion, rather the very little volatile loss after torrefaction had changed the mechanism to power law.

Reaction mechanism at lower conversion (α>0.5). From 0.5 to 0.9, conversion of the raw and torrefied EFB occurs at higher degree with more complex reaction mechanism (*Table 3*). At conversion above 0.5, the raw biomass follows power law (P3 and P4) mechanism (Postawa *et al.*, 2022). This transition, from diffusion to power law mechanism was accomplished due to massive loss of volatile matter at conversion less than 0.5. In addition, to the power law (P3 and P4) torrefied EFB_T-225 could also experience 3rd order random nucleation (contracting volume, R3) with three nuclei on each particle, while EFB_T-250 could advance further into nucleation and growth pathway, A4 by Avrami-Erofeev model. Torrefied EFB_T-300 could also be described by Avrami-Erofeev models (A1, A3, and A4) for nucleation and growth mechanisms. At higher temperature, relatively higher conversion of biomass could occur due to an accelerated decomposition. Moreover, cleavage of some larger ordered cellulose into lower molecular mass chain could occur, which then facilitates the nucleation, growth and decomposition processes (Singh *et al.*, 2020b) .

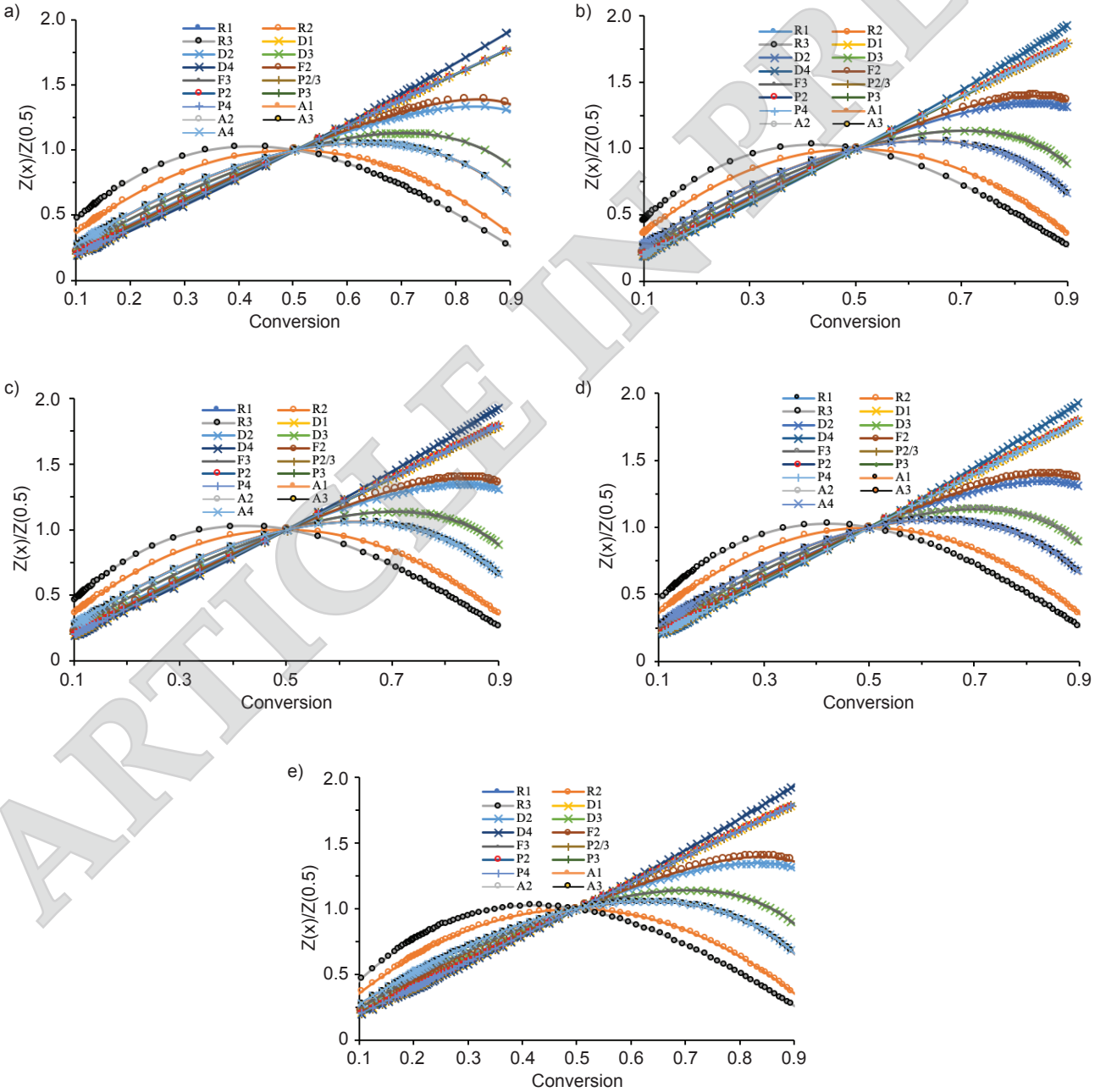

Figure 7. Theoretical and experimental plots for prediction of solid-state reaction mechanism using Criado method (Z-master plot). a) Raw_EFB, b) EFB_T-225, c) EFB-T250, d) EFB_T-275 and e) EFB_T-300.

TABLE 3. PREDICTED MODELS FOR RAW AND TORREFIED EMPTY FRUIT BUNCHES

Biomass	Solid state	
	Conversion less than 0.5	Conversion greater than 0.5
Raw EFB	Diffusion model D3(0.9994) D3 $f(\alpha) = 3/2(1-\alpha)^{2/3}[1-(1-\alpha)^{1/3}]^{-1}$ $g(\alpha) = [1-(1-\alpha)^{1/3}]^2$	Power Law models P3(0.9859), P4(0.9928) P3 $f(\alpha) = 3\alpha^{2/3}$, $g(\alpha) = \alpha^{1/3}$ P4 $f(\alpha) = 4\alpha^{3/4}$, $g(\alpha) = \alpha^{1/4}$
EFB_T-225	Power Law models P4(0.9487) P4 $f(\alpha) = 4\alpha^{3/4}$, $g(\alpha) = \alpha^{1/4}$	Power Law models P3(0.9667), P4(0.9807) P3 $f(\alpha) = 3\alpha^{2/3}$, $g(\alpha) = \alpha^{1/3}$ P4 $f(\alpha) = 4\alpha^{3/4}$, $g(\alpha) = \alpha^{1/4}$
EFB_T-250	Power Law models P4(0.9716) P4 $f(\alpha) = 4\alpha^{3/4}$, $g(\alpha) = \alpha^{1/4}$	Power Law models P3 (0.9762), P4 (0.9856) P3 $f(\alpha) = 3\alpha^{2/3}$, $g(\alpha) = \alpha^{1/3}$ P4 $f(\alpha) = 4\alpha^{3/4}$, $g(\alpha) = \alpha^{1/4}$ 3rd order random nucleation having three nucleus on individual particle R3 (0.9779) $f(\alpha) = (1-\alpha)^3$ $g(\alpha) = 1/2[(1-\alpha)^{-2}-1]$
EFB_T-275	P4(0.9735), P4 $f(\alpha) = 4\alpha^{3/4}$, $g(\alpha) = \alpha^{1/4}$ Avrami-Erofeev models, A4(0.9625) A4 $f(\alpha) = 4(1-\alpha)[-\ln(1-\alpha)]^{3/4}$ $g(\alpha) = [-\ln(1-\alpha)]^{1/4}$	P3(0.9716), P4(0.9716), P3 $f(\alpha) = 3\alpha^{2/3}$, $g(\alpha) = \alpha^{1/3}$ P4 $f(\alpha) = 4\alpha^{3/4}$, $g(\alpha) = \alpha^{1/4}$ Avrami-Erofeev models, A4(0.9894) A4 $f(\alpha) = 4(1-\alpha)[-\ln(1-\alpha)]^{3/4}$ $g(\alpha) = [-\ln(1-\alpha)]^{1/4}$
EFB_T-300	Power Law models P3 (0.9886), P4(0.9921), P3 $f(\alpha) = 3\alpha^{2/3}$, $g(\alpha) = \alpha^{1/3}$ P4 $f(\alpha) = 4\alpha^{3/4}$, $g(\alpha) = \alpha^{1/4}$ A3(0.9846), A4(0.9915) A3 $f(\alpha) = 3(1-\alpha)[-\ln(1-\alpha)]^{2/3}$ $g(\alpha) = [-\ln(1-\alpha)]^{1/3}$ A4 $f(\alpha) = 4(1-\alpha)[-\ln(1-\alpha)]^{3/4}$	Power Law models P3 (0.9871), P4(0.992), P3 $f(\alpha) = 3\alpha^{2/3}$, $g(\alpha) = \alpha^{1/3}$ P4 $f(\alpha) = 4\alpha^{3/4}$, $g(\alpha) = \alpha^{1/4}$ Avrami-Erofeev models, A1(0.9898), A3(0.9888), A4(0.9947) A1 $f(\alpha) = 1/2(1-\alpha)[-\ln(1-\alpha)]^{1/3}$ $g(\alpha) = [-\ln(1-\alpha)]^{2/3}$ A3 $f(\alpha) = 3(1-\alpha)[-\ln(1-\alpha)]^{2/3}$ $g(\alpha) = [-\ln(1-\alpha)]^{1/3}$ A4 $f(\alpha) = 4(1-\alpha)[-\ln(1-\alpha)]^{3/4}$ $g(\alpha) = [-\ln(1-\alpha)]^{1/4}$

Note: EFB T-XXX = EFB torrefied at XXX°C.

CONCLUSION

In this study, torrefaction was performed on EFB before subjecting it to pyrolysis. Torrefaction was able to improve the physiochemical properties of raw EFB, and alter the chemical composition in such to be deemed desirable for pyrolysis with lower activation energy required. The fuel quality (volatile matter, H/C, O/C and CV) of the torrefied EFB had been greatly enhanced, while thermal stability decreased with temperature. The activation energy of hemicellulose, cellulose and lignin of the torrefied EFB decreased with increasing pyrolysis degradation temperature. The thermal degradation of torrefied individual component and the whole EFB was in the order of hemicellulose > cellulose > lignin, and EFB_T-300 > EFB_T-275 > EFB_T-250 > EFB_T-225 > raw EFB. These findings suggested that torrefied EFB could be a better solid fuel as torrefaction is able to convert the power law mechanism to nucleation and gradual growth mechanism, which eases decomposition during combustion. Overall, it can be concluded that torrefied EFB is a potential feedstock for bio-energy production.

ACKNOWLEDGEMENT

The authors would like to thank the Director-General of MPOB for permission to publish this article.

REFERENCES

Abnisa, F and Alaba, P A (2021). Recovery of liquid fuel from fossil-based solid wastes via pyrolysis technique: A review. *J. Environ. Chem. Eng.*, 106593.

Alaba, P A; Popoola, S I; Abnisal, F; Lee, C S; Ohunakin, O S; Adetiba, E; Akanle, M B; Patah, M F A; Atayero, A A and Daud, W M A W (2020). Thermal decomposition of rice husk: A comprehensive artificial intelligence predictive model. *J. Therm. Anal. Calorim., 140(4)*: 1811-1823.

Alaba, P A; Sani, Y M and Daud, W M A W (2016). A comparative study on thermal decomposition behavior of biodiesel samples produced from shea butter over micro- and mesoporous ZSM-5 zeolites

using different kinetic models. *J. Therm. Anal. Calorim.*, *126(2)*: 943-948.

Almeida, G; Brito, J and Perré, P (2010). Alterations in energy properties of eucalyptus wood and bark subjected to torrefaction: The potential of mass loss as a synthetic indicator. *Bioresour. Technol.*, *101(24)*: 9778-9784.

ASTM (1978a). Designation: D 1104-56. Method of test for holocellulose in wood. ASTM International, West Conshohocken.

ASTM (1978b). Designation: D 1103-60. Standard test method for α-cellulose. ASTM International, West Conshohocken.

ASTM (1998). Designation: D 5142. Standard test methods for proximate analysis of the analysis sample of coal and coke by instrumental procedures. ASTM International, West Conshohocken.

ASTM (2014). Designation: D 5373. Standard test methods for determination of carbon, hydrogen and nitrogen in analysis samples of coal and carbon in analysis samples of coal and coke. ASTM International, West Conshohocken.

ASTM (2019). Designation: D 5865. Standard test method for gross calorific value of coal and coke. ASTM International, West Conshohocken.

ASTM (2020). Designation: E 1131. Standard test method for compositional analysis by thermogravimetry. ASTM International, West Conshohocken.

Brillard, A; Trouvé, G; Maryandyshev, P; Kehrli, D; Lyubov, V and Brilhac, J F (2020). Analysis through thermogravimetric analyses of the impact of torrefaction processes performed under a non-oxidative atmosphere on hydrolysis lignin samples. *Fuel*, *260*: 116261.

Chang, S H (2014). An overview of empty fruit bunch from oil palm as feedstock for bio-oil production. *Biomass Bioenergy*, *62*: 174-181.

Chen, D; Chen, F; Cen, K; Cao, X; Zhang, J and Zhou, J (2020). Upgrading rice husk via oxidative torrefaction: Characterization of solid, liquid, gaseous products and a comparison with non-oxidative torrefaction. *Fuel*, *275*: 117936.

Chen, D; Gao, A; Ma, Z; Fei, D; Chang, Y and Shen, C (2018). In-depth study of rice husk torrefaction: Characterization of solid, liquid and gaseous products, oxygen migration and energy yield. *Bioresour. Technol.*, *253*: 148-153.

Chiou, B S; Valenzuela-Medina, D; Bilbao-Sainz, C; Klamczynski, A K; Avena-Bustillos, R J; Milczarek, R R; Du, W X; Glenn, G M and Orts, W J (2015). Torrefaction of pomaces and nut shells. *Bioresour. Technol.*, *177*: 58-65.

Criado, J M (1978). Kinetic analysis of DTG data from master curves. *Thermochimica Acta*, *24(1)*: 186-189.

Damartzis, T; Vamvuka, D; Sfakiotakis, S and Zabaniotou, A (2011). Thermal degradation studies and kinetic modeling of cardoon (*Cynara cardunculus*) pyrolysis using thermogravimetric analysis (TGA). *Bioresour. Technol.*, *102(10)*: 6230-6238.

Fleig, O P; Raymundo, L M; Trierweiler, L F and Trierweiler, J O (2021). Study of rice husk continuous torrefaction as a pretreatment for fast pyrolysis. *J. Anal. Appl. Pyrolysis*, *154*: 104994.

Gogoi, M; Konwar, K; Bhuyan, N; Borah, R C; Kalita, A C; Nath, H P and Saikia, N (2018). Assessments of pyrolysis kinetics and mechanisms of biomass residues using thermogravimetry. *Bioresour. Technol. Rep.*, *4*: 40-49.

Kasim, N N; Ismail, K; Mohamed, A R; Ishak, M A M; Ahmad, R; Nawawi, W I and Ismail, W (2018). Characteristic, thermochemical behaviors and kinetic of demineralized and torrefied empty fruit bunches (EFB). *Adv. Sci. Technol. Eng. Syst. J.*, *3(5)*: 365-373.

Kumar Mishra, R and Mohanty, K (2021). Kinetic analysis and pyrolysis behavior of low-value waste lignocellulosic biomass for its bioenergy potential using thermogravimetric analyzer. *Materials Science for Energy Technologies*, *4*: 136-147.

Li, Z; Zhao, W; Meng, B; Liu, C; Zhu, Q and Zhao, G (2008). Kinetic study of corn straw pyrolysis: Comparison of two different three-pseudocomponent models. *Bioresour. Technol.*, *99(16)*: 7616-7622.

Loh, S K (2017). The potential of the Malaysian oil palm biomass as a renewable energy source. *Energy Convers. Manag.*, *141*: 285-298.

Luo, L; Zhang, Z; Li, C; He, F; Zhang, X and Cai, J (2021). Insight into master plots method for kinetic analysis of lignocellulosic biomass pyrolysis. *Energy*, *233*: 121194.

Mohamed, A R; Li, N; Ahmad Sohaimi, K S; Iberahim, N I; Rohaizad, N M and Hamzah, R (2018). Kinetic parameters of non-isothermal thermogravimetric non-catalytic and catalytic pyrolysis of empty

fruit bunch with alumina by Kissinger and Ozawa methods. *IOP Conf. Ser.: Mater. Sci. Eng.*, *318*: 012019.

Müller-Hagedorn, M and Bockhorn, H (2007). Pyrolytic behaviour of different biomasses (angiosperms) (maize plants, straws, and wood) in low temperature pyrolysis. *J. Anal. Appl. Pyrolysis*, *79(1)*: 136-146.

Nudri, N A; Bachmann, R T; Ghani, W A W A K; Sum, D N K and Azni, A A (2020). Characterization of oil palm trunk biocoal and its suitability for solid fuel applications. *Biomass Convers. Biorefin.*, *10(1)*: 45-55.

Parveez, G K A; Tarmizi, A H A; Sundram, S; Loh, S K; Ong-Abdullah, M; Palam, K D P; Salleh, K M; Ishak, S M and Idris, Z (2021). Oil palm economic performance in Malaysia and R&D progress in 2020. *J. Oil Palm Res.*, *33(2)*: 181-214.

Postawa, K; Fałtynowicz, H; Szczygieł, J; Beran, E and Kułażyński, M (2022). Analyzing the kinetics of waste plant biomass pyrolysis via thermogravimetry modeling and semi-statistical methods. *Bioresour. Technol.*, *344*: 12618.

Sharma, R and Sheth, P N (2018). Multi reaction apparent kinetic scheme for the pyrolysis of large size biomass particles using macro-TGA. *Energy*, *151*: 1007-1017.

Singh, R K; Chakraborty, J P and Sarkar, A (2020a). Optimizing the torrefaction of pigeon pea stalk (*Cajanus cajan*) using response surface methodology (RSM) and characterization of solid, liquid and gaseous products. *Renew. Energ.*, *155*: 677-690.

Singh, R K; Sarkar, A and Chakraborty, J P (2019). Effect of torrefaction on the physicochemical properties of pigeon pea stalk (*Cajanus cajan*) and estimation of kinetic parameters. *Renew. Energ.*, *138*: 805-819.

Singh, S; Prasad Chakraborty, J and Kumar Mondal, M (2020b). Intrinsic kinetics, thermodynamic parameters and reaction mechanism of non-isothermal degradation of torrefied *Acacia nilotica* using isoconversional methods. *Fuel*, *259*: 116263.

Soh, M; Chew, J J; Liu, S and Sunarso, J (2019). Comprehensive kinetic study on the pyrolysis and combustion behaviours of five oil palm biomass by thermogravimetric-mass spectrometry (TG-MS) analyses. *BioEnergy Res.*, *12(2)*: 370-387.

Sukiran, M A; Abnisa, F; Syafiie, S; Wan Daud, W M A; Nasrin, A B; Abdul Aziz, A and Loh, S K (2020). Experimental and modelling study of the torrefaction of empty fruit bunches as a potential fuel for palm oil mill boilers. *Biomass Bioenergy*, *136*: 105530.

Sukiran, M A; Abnisa, F; Wan Daud, W M A; Abu Bakar, N and Loh, S K (2017). A review of torrefaction of oil palm solid wastes for biofuel production. *Energy Convers. Manag.*, *149*: 101-120.

Sukiran, M A; Wan Daud, W M A; Abnisa, F; Nasrin, A B; Abdul Aziz, A and Loh, S K (2021). A comprehensive study on torrefaction of empty fruit bunches: Characterization of solid, liquid and gas products. *Energy*, *230*: 120877.

Surahmanto, F; Saptoadi, H; Sulistyo, H and Rohmat, T A (2020). Investigation of the pyrolysis characteristics and kinetics of oil-palm solid waste by using Coats-Redfern method. *Energy Explor. Exploit.*, *38(1)*: 298-309.

TAPPI (2011). Designation: T222 om-11. Acid-insoluble lignin in wood and pulp. TAPPI Press, Atlanta, GA.

Tian, X; Dai, L; Wang, Y; Zeng, Z; Zhang, S; Jiang, L; Yang, X; Yue, L; Liu, Y and Ruan, R (2020). Influence of torrefaction pretreatment on corncobs: A study on fundamental characteristics, thermal behavior, and kinetic. *Bioresour. Technol.*, *297*: 122490.

Wang, L; Barta-Rajnai, E; Skreiberg, Ø; Khalil, R; Czégény, Z; Jakab, E; Barta, Z and Grønli, M (2018). Effect of torrefaction on physiochemical characteristics and grindability of stem wood, stump and bark. *Appl. Energy*, *227*: 137-148.

Wang, L; Barta-Rajnai, E; Skreiberg, Ø; Khalil, R; Czégény, Z; Jakab, E; Barta, Z and Grønli, M (2017). Impact of torrefaction on woody biomass properties. *Energy Procedia*, *105*: 1149-1154.

Zhang, J and Zhang, X (2019). The thermochemical conversion of biomass into biofuels. *Biomass, Biopolymer-Based Materials, and Bioenergy*. Elsevier. p. 327-368.

Zhang, R; Zhang, J; Guo, W; Wu, Z; Wang, Z; Yang, B (2021). Effect of torrefaction pretreatment on biomass chemical looping gasification (BCLG) characteristics: Gaseous products distribution and kinetic analysis. *Energy Conver. Manag.*, *237*: 114100.